Brain Structure and Function (2020) 225:1389–1400
https://doi.org/10.1007/s00429-019-02013-5

ORIGINAL ARTICLE

A generic brain connectome map linked to different types of everyday decision-making in old age

Brian Rooks[1,2] · Mia Anthony[2,4] · Quanjing Chen[2,3] · Ying Lin[4] · Timothy Baran[5,6] · Zhengwu Zhang[1,7] · Peter A. Lichtenberg[8] · Feng Lin[2,3,4,7,9]

Received: 26 July 2019 / Accepted: 14 December 2019 / Published online: 19 December 2019

Abstract

Making reasonable decisions related to financial and health scenarios is a crucial capacity that can be difficult for older adults to maintain as they age, yet few studies examine neurocognitive factors that are generalizable to different types of everyday decision-making capacity. Here we propose an innovative approach, based on individual risk-taking preference, to identify neural profiles that may help predict older adults' everyday decision-making capacity. Using performance and cognitive arousal information from two gambling tasks, we identified three decision-making preference groups: ambiguity problem-solvers (A), risk-seekers (R), and a control group without strong risk-taking preferences (C). Comparisons of the number of connections within white matter tracts between A vs. C and R vs. C groups resulted in features consistent with the theory of dual neural functional systems involved in decision-making. Unique tracts from the A vs. C contrast were primarily centered in dorsal frontal regions/reflective system; unique tracts from the R vs. C contrast were centered in the ventral frontal regions/impulsive system; and shared tracts from both contrasts were centered in the basal ganglia, coordinating the switch between the two types of decision-making preference. Number of connections from the tracts differentiating A vs. C significantly predicted financial and health/safety decision-making capacity, and the association remained significant after controlling for multiple socioeconomic and cognitive factors. The connectome identified may provide insight into a generic white matter mechanism related to everyday decision-making capacity in older age.

Keywords Everyday decision-making · Connectome · White matter · Aging · Gambling task

Brian Rooks and Mia Anthony contributed equally.

Electronic supplementary material The online version of this article (https://doi.org/10.1007/s00429-019-02013-5) contains supplementary material, which is available to authorized users.

✉ Brian Rooks
Brian_Rooks@urmc.rochester.edu

✉ Feng Lin
FengVankee_Lin@urmc.rochester.edu

[1] Department of Biostatistics and Computational Biology, School of Medicine and Dentistry, University of Rochester Medical Center, Rochester, USA

[2] Elaine C. Hubbard Center for Nursing Research On Aging, School of Nursing, University of Rochester Medical Center, Rochester, NY, USA

[3] Department of Psychiatry, School of Medicine and Dentistry, University of Rochester Medical Center, Rochester, USA

[4] Department of Brain and Cognitive Sciences, University of Rochester, Rochester, USA

[5] Department of Imaging Science, School of Medicine and Dentistry, University of Rochester Medical Center, Rochester, USA

[6] Department of Biomedical Engineering, University of Rochester, Rochester, USA

[7] Department of Neuroscience, School of Medicine and Dentistry, University of Rochester Medical Center, Rochester, USA

[8] Institute of Gerontology, Wayne State University, Detroit, USA

[9] Department of Neurology, School of Medicine and Dentistry, University of Rochester Medical Center, Rochester, USA

Introduction

Making reasonable decisions related to financial and health scenarios is a crucial capacity that can be difficult for older adults to maintain as they age. Investigating neurocognitive factors that contribute to decision-making capacity in older adults pertaining to these everyday life-related scenarios is important for both researchers and clinicians to develop preventative strategies appropriate for addressing behavioral issues that manifest during the decision-making process (Samanez-Larkin et al. 2010; Han et al. 2016; Spreng et al. 2017). However, whether the same set of neural profiles in old age can explain the capacities for different types of everyday decision-making is understudied.

There are two types of behaviors or strategies involved in risk-taking—known probability (referred here as "risk") and unknown probability (referred here as "ambiguity"). The difference between known vs. unknown probability is reflected in the presence or absence of explicit information about their rules and associated consequences, as well as the probability between them (Liebherr et al. 2017). Individuals who prefer risk-based strategies are excited by risk-taking behavior and thus more willing to take risks, while individuals who prefer ambiguity-based strategies tend to exhibit a bias towards problem-solving and can become fatigued from sustaining cognitive processes that support pattern evaluation (Liebherr et al. 2017). Although the concrete strategies individuals employ for different types of everyday decision-making may vary, depending on the scenario, the underlying risk-taking preference can become inflexible with age, a process that is sensitive to lifetime factors (e.g., socioeconomic status, culture, insight gained from previous decisions, personality, cognitive and physical health) (Li et al. 2004; Mikels et al. 2013). Furthermore, there exists evidence that experiential, behavioral, and physiological factors shape over time an individual's white matter structural connectome (Giedd and Rapoport 2010). These connectomes facilitate communication that emerges from dynamic information processing on the neural functional level and show less acute event-induced change compared to neural function (Monje 2018). Finally, recent studies on healthy young adults have implicated that the integrity of specific white matter tracts contributes to the magnitude of impulsive risk-taking behaviors. The anterior insula-nucleus accumbens tract has been associated with preferences for positively skewed gambling behavior (Leong et al. 2016); tracts between ventral striatum and ventromedial or dorsolateral prefrontal cortex (PFC) have been implicated in reward impulsivity (Hampton et al. 2017); and tracts linking PFC, insula, midbrain, and striatum have been linked to the number of risky decisions an individual makes on a gambling task (Kohno et al. 2017). Convergence of these lines of evidence presents the possibility that the integrity of specific subsets of tracts can be indicative of decision-making capacity.

To our knowledge, no study has investigated associations between white matter integrity and decision-making in a sample of exclusively older adults, who tend to use reflective processing (a top-down process driven by cognition) in their decision-making more than younger adults (Schiebener and Brand 2015). Synthesizing cumulative literature, we suspect connectomes underlying risk-taking preference may be a useful neural profile for predicting capacities associated with different types of everyday decision-making in old age.

Our goal was to identify a neural profile, indexed by white matter connectomes representing different risk-taking preferences, that is predictive of decision-making in older adults across different everyday scenarios. We first categorized cognitively typical older adults based on their risk-taking preference**.** We utilized two gambling tasks requiring implicit learning of potential outcomes [Iowa Gambling Task (IGT), and Balloon Analogue Risk Task (BART)], where optimal performance relies on either risk-aversion (IGT) or risk-taking (BART) (Mata et al. 2011). In addition, cognitive arousal was quantified by comparing individuals' self-appraisal of their mental status immediately before and after the gambling tasks. We hypothesized that individuals who performed well but became fatigued on both IGT and BART to be those who prefer ambiguity-based strategies (A); individuals who performed well on BART but poorly on IGT and experienced concomitant cognitive arousal to be those who prefer risk-based strategies (R); and individuals who did not perform well on either task, suggesting an absence of strong risk-taking preference, to be a control group (C). Next, we compared connectomes between risk-taking preference types. Adopting the theory of dual neural functional systems involved in decision-making (Schiebener and Brand 2015), we proposed that connectomes underlying risk-based preference would overlap with the impulsive system (primarily through the amygdala, ventral striatum, and orbitofrontal cortex), while connectomes underlying ambiguity-based preference would overlap with the reflective system (primarily through the dorsolateral prefrontal cortex, anterior cingulate cortex, and posterior parietal cortex). A subset of connectomes, however, were predicted to be shared by the two risk-taking preference types and align with regions involved in the coordination system (basal ganglia-oriented). Finally, we examined the relationship between risk-taking preferences, as well as their underlying connectomes, and perceived everyday decision-making capacity. Since decision-making typically involves a combination of risk and ambiguity, we hypothesized that connectomes supporting the coordination system would have the highest

predictive value for the way in which individuals perceive their capacity for everyday decision-making compared to connectomes related to a specific risk-taking preference (A only or R only).

Methods

Sample description

Fifty-two physically healthy older adults were recruited (mean age = 71 ± 5.12, 69.2% female, years of education = 17 ± 2.81) with normal cognition, as defined by Montreal Cognitive Assessment (MoCA) ≥ 26 and Rey's Auditory Verbal Learning Test (RAVLT) delayed recall ≥ 6. Inclusion criteria included: (1) intact capacity to give consent (assessed using UCSD Brief Assessment of Capacity to Consent); (2) adequate visual and auditory acuity for testing by self-report; (3) absence of major depression (Geriatric Depression Scale-15 item score < 6), sleep disorders (Pittsburgh Sleep Quality Inventory global sleep quality score < 14), and chronic fatigue (20-item Multidimensional Fatigue Inventory general fatigue subscale < 20); (4) ≥ 65 years of age; (5) English-speaking; and (6) community-dwelling. Exclusion criteria included: (1) neurologic or vascular disorders (e.g., multiple sclerosis, stroke, transient ischemic attack, heart attack, or traumatic brain injury within the past 5 years; severe cerebrovascular disease, Parkinson's disease); (2) an episode of a diagnosed and active psychiatric disorder (i.e., major depression, anxiety, bipolar disorder) within the past 5 years; (3) schizophrenia (regardless of the time from which the last episode occurred); (4) clinical diagnosis of mild cognitive impairment or dementia, as defined by the most current version of DSM; (5) MRI contraindications (e.g., pacemaker, metallic implant, claustrophobia). The study was approved by the Institutional Review Board of University of Rochester. All participants provided written consent.

Study design

A cross-sectional observational study was conducted. Data on diffusion tensor imaging (DTI), two gambling tasks (IGT and BART), self-report everyday decision-making capacity, and cognitive function were collected.

Assessment of everyday decision-making capacity

Two self-report measures were used. The Lichtenberg Financial Decision-Making Rating Scale (LFDRS) was used to quantify perceived financial decision-making capacity; and the Likelihood subscale of the Domain-Specific Risk-Taking (DOSPERT) scale was used to assess multiple domains of everyday decision-making capacity, including the financial domain.

LFDRS consists of four subscales that quantify contextual factors, defined by the authors as variables specific to financial decision-making: Financial Situation Awareness (e.g., How worried are you about having enough money to pay for things?); Psychological Vulnerability (e.g., How often do you wish that you had someone to talk to about finances?); and Susceptibility (to Undue Influence or Financial Exploitation) (e.g., Has a relationship with a family member or friend become strained due to finances as you have grown older?). An additional subscale quantifies Intellectual Factors, defined as variables fundamental to financial decisional capacity, specifically choice, rationale, understanding, and appreciation (total of 7 items) (Lichtenberg et al. 2018b). LFDRS has been validated in several aging populations (Lichtenberg et al. 2016, 2018a). Cronbach's alpha across all items was 0.71 in the current study. Participant responses were coded ordinally based on risk (0–4, a lower score indicating lower risk), then summed to calculate a risk score for each contextual subscale and Intellectual Factors, yielding a total of five risk scores for each participant. Contextual factor composite risk scores were calculated using a subset of 23 items (7 Financial Situation Awareness items, 8 Psychological Vulnerability items, and 6 Susceptibility items) [for item selection, see (Lichtenberg et al. 2017)]. A total LFDRS score was calculated as the average of the contextual and intellectual composite scores, with higher scores indicating greater vulnerability to financial incapacity.

The Likelihood subscale of the DOSPERT (Blais and Weber 2006) asks participants to rate their perceived likelihood of engaging in 30 different hypothetical activities using a 7-item Likert scale (1, "extremely unlikely" and 7, "extremely likely"). Activities are categorized into five domains: 1) health/safety (e.g., driving a car without a seatbelt, engaging in unprotected sex); 2) ethical (e.g., taking questionable deductions on income tax return); 3) social (e.g., admitting tastes different from a friend); 4) financial (e.g., investment, gambling); and 5) recreational (e.g., taking a skydiving class. A total likelihood score for each participant was computed as the sum of all item ratings, with higher scores indicating a higher likelihood of engaging in the activities. Domain-specific scores were calculated as the sum of item ratings for a given domain, with higher scores indicating a higher risk-taking attitude. Cronbach's alpha across all domains was > 0.70.

Of note, there was a significant correlation between the LFDRS and DOSPERT financial score ($r = 0.36$, $p = 0.030$) in the current study.

Gambling task protocols

Participants completed two gambling tasks, IGT and BART, between 8 am and 12 pm. Participants were instructed to eat breakfast but to avoid nicotine, caffeine, and exercise for at least 2 h prior to arrival. The two gambling tasks, randomized in order across participants, lasted 30 min (15 min per task). Upon arrival, participants rested for 5 min, then rated their pre-task cognitive arousal using an 18-item Visual Analogue Scale (VAS). The VAS was adapted from the original version (Lee et al. 1991), using a Likert scale ranging from 0 ("not at all") to 10 ("very much"). Participants were instructed to rate their current state of cognitive arousal based on terms related to mood and energy (e.g., tired, keeping your eyes open is difficult, lively, efficient). Immediately after the tasks, participants rated their post-task cognitive arousal once more using the same VAS. Differences in ratings before and after performing IGT and BART were averaged over all 18 items to compute a single cognitive arousal score for each participant. Higher positive scores indicated lower post-task cognitive arousal, while lower negative scores indicated higher cognitive arousal.

During IGT, participants were presented with four virtual decks of cards (A, B, C, and D) and were instructed to select or "play" decks to maximize profit. Decks yielded either high immediate gains with larger future losses (risky decks, A and B) or low immediate gains with smaller future losses (safe decks, C and D). After each deck selection, a random amount of money based on the deck type was awarded to or deducted from participants' total winnings. Higher performance was achieved by participants who played the safe decks at a higher rate than the risky decks.

During BART, participants were presented with a virtual balloon on the screen and instructed to "pump" the balloon to earn monetary rewards. Each pump inflated the balloon larger, thereby increasing not only the amount of money a participant could potentially collect but also the probability of "popping" the balloon and forfeiting the reward. The balloons were presented in three different colors (red, yellow, and blue), which corresponded to the maximum number of times a balloon could be pumped before exploding, as well as the likelihood of exploding for any number of pumps. Red balloons were assigned the highest conditional probability of exploding on any given pump and therefore yielded the lowest reward potential; blue balloons were assigned the lowest conditional probability of exploding and yielded the highest reward potential; and yellow balloons were assigned a conditional probability of exploding and a reward potential in between those of red and blue. Higher performance was achieved by individuals who were willing to take greater risks (i.e., greater number of pumps) to increase their reward potential.

Participants were instructed to maximize their rewards in each trial while avoiding losses but were not given prior information about the relative risks or reward/loss potentials associated with the IGT decks or BART balloons, respectively.

Cumulatively, IGT requires participants to resist playing the initially attractive decks with high-risk but negative expected value in favor of the less attractive decks with low-risk but positive expected value. In contrast, BART rewards participants who delay their decision to collect a given reward in favor of a larger reward potential, despite the increase in risk. For each participant, an overall task performance score was computed for IGT and BART separately. The IGT performance score was calculated as the proportion of times a participant played a safe deck (C or D) minus the proportion of times a participant played a risky deck (A or B). The BART performance score was calculated as the weighted average of a participant's earnings from the red, yellow, and blue balloon trials, with weights corresponding to the proportion of each color among the unexploded balloon trials. For both task performance scores, higher values were interpreted as better overall decision-making on the given task. Additionally, higher IGT performance specifically indexed lower risk-seeking behavior, while higher BART performance indexed higher risk-seeking behavior (Zamarian et al. 2011; Koscielniak et al. 2016).

Risk-taking preference cluster determination

To derive connectome-based features that reflect differences in risk-taking preferences, we first used k-means clustering to divide the participants into groups according to their IGT, BART, and cognitive arousal z-scores. Out of the 52 participants, two were excluded from the clustering analyses due to technical errors while recording their gambling behavior data. The clustering procedure yielded three groups, which we will refer to as (1) a group preferring ambiguity-based decision-making (A), (2) a control group with no apparent risk-taking preference (C), and (3) a group preferring risk-based decision-making (R). The contrasts of interest for obtaining features were A vs. C and R vs. C.

Neurocognitive covariates

Cognitive measures of interest included total score on MoCA, a measure of global cognition; cognitive control and working memory factor scores from EXAMINER, a test of executive function; delayed recall obtained from RAVLT, a measure of episodic memory; and performance on Wisconsin Card Sorting Test (WCST), a test of reasoning and problem-solving ability. Brain pathology was operationalized as a participant's average cortical thickness over the whole brain.

Image acquisition

Data were collected at the Rochester Center for Brain Imaging using a 3 T Siemens Trio TIM scanner (Erlangen, Germany) equipped with a 32-channel receive-only head coil transmission. Each MRI session began with a scout image, followed by an MPRAGE scan (TR/TE = 2530/3.44 ms, TI = 1100 ms, FA = 7, matrix = 256 × 256, resolution 1 × 1 × 1 mm^3, 192 slices). DTI was performed using a 2D axial single-short dual-echo SE-EPI sequence with TR/TE = 8900/86 ms, matrix = 128 × 128, FOV = 256 × 256 mm^2, 2 mm slice thickness with no gap (60 slices for whole brain coverage), iPAT (GRAPPA) acceleration factor = 2, DW direction = 60 with b = 1000 s/mm^2 and 1 average, and b = 0 images with 10 averages.

DTI preprocessing

DTI data were first corrected for eddy current-induced distortion, motion, and susceptibility-induced distortion. Corrected data were then processed using the population-based structural connectome pipeline, which has been described in detail previously (Zhang et al. 2018). Briefly, this pipeline performs HARDI tractography with anatomical priors, then registers this data to parcellated T1 data for the same subject and groups each tractography dataset into bundles connecting specified regions of interest. Characteristics of these streamline bundles can then be used to generate connectome matrices for each subject for a number of metrics, where each element of the connectome matrix represents a particular measure along the connection between two regions of interest. We argue that analyzing connectome data from the PSC pipeline has two advantages over traditional voxel-based analyses of diffusion metrics. First, the PSC pipeline explicitly models the geometry of fiber bundles prior to computing diffusion metrics and allows one to compute diffusion metrics along tracts of interest, which may provide greater specificity of diffusion summary measures for a given fiber tract than one could obtain from voxel-based analyses. Second, the PSC pipeline performs parcellation and computes diffusion metrics in each subject's native space without the need to deform each subject's diffusion metric image to a common template, as in TBSS. Here, we primarily focused on total number of connections, which represents the number of streamlines connecting two regions, because connectomes of the number of connections have been shown to have greater within-subject reproducibility than connectomes of anisotropy or diffusivity (Zhang et al. 2018), suggesting that these connectome matrices provide fingerprints of a subject's white matter structure while summarizing tract properties between ROIs. We will subsequently refer to the number of connections as connectivity. The total number of streamlines in participants' tractography datasets before segmentation ranged from 1.17 to 1.55 million streamlines, with a mean ± SD of 1.36 ± 0.10 million streamlines. Additionally, we computed connectomes containing average fractional anisotropy (FA) and average mean diffusivity (MD) along ROI-to-ROI tracts, as well as the proportion of streamlines between ROIs relative to the total number of whole-brain streamlines. Results from the prediction analyses of LFDRS and DOSPERT scores using these alternative connectome measures can be found in Supplementary Tables 1–3. The results of the prediction analyses for mean FA and mean MD were very weak or similar to those using connectivity as the connectome measure (i.e., proportion of total streamlines); thus, the subsequent feature selection and results sections are restricted to the analyses using connectivity as the connectome measure.

ROIs consisted of 68 cortical regions, 18 subcortical regions, and a brainstem region, using the Desikan-Killiany atlas (Desikan et al. 2006). Parcellation was performed with FreeSurfer (v6.0.0, surfer.nmr.mgh.harvard.edu/fswiki/FreeSurferWiki). After preprocessing, each subject had an 87-by-87 matrix containing the connectivity for every ROI pair.

Feature selection

Tracts were selected as features by thresholding Kendall's tau statistics comparing the connectome measures from the A or R group to the connectome measures from the C group. Given observations $X_{11}, \ldots X_{1n_1}$ from group 1 and $X_{21}, \ldots X_{2n_2}$ from group 2, the Kendall's tau statistic comparing group 1 to group 2 is computed as

$$\tau = \frac{\sum_{i=1}^{n_1} \sum_{j=1}^{n_2} \operatorname{sign}\left(X_{1i} - X_{2j}\right)}{n_1 n_2},$$

where $\operatorname{sign}\left(X_{1i} - X_{2j}\right) = 1$ if $X_{1i} > X_{2j}$, −1 if $X_{1i} < X_{2j}$, or 0 if $X_{1i} = X_{2j}$. The tau statistic lies between -1 and 1 and provides a measure of separation between two groups based on their relative ranks. If every observation from group 1 is larger (smaller) than every observation from group 2, τ will equal 1 (− 1). In general, a statistic equal to τ means that, on average, an observation from group 1 is larger than $0.5 \times (1 + \tau) \times 100\%$ percent of observations from group 2. For example, obtaining a tau statistic of 0.50 means that on average, an observation from group 1 is larger than 75% of the observations from group 2. We used the non-parametric Kendall's tau test to compare tract measures between the groups because we anticipated that we likely needed to transform the tract measurements to reduce skewness. Furthermore, unlike traditional two-sample t-test statistics, the tau statistic is invariant under monotonic transformations (e.g., logarithmic and square root).

For the contrasts A vs. C and R vs. C, we computed the Kendall's tau statistic at every ROI pair/tract for

connectivity. A tract was excluded from the set of candidate features if fewer than 75% of participants had a nonzero connectivity for that tract. A two-sided hypothesis test of the null hypothesis that $\tau = 0$ was carried out for each candidate feature, with tracts selected as features if their tau statistic was significantly different from 0 at alpha level 0.05. The cutoff used for conducting the hypothesis test was

$$\frac{z_{0.975}}{\sqrt{3nc(1-c)}},$$

where $z_{0.975} \approx 1.96$ is the 97.5th percentile of the standard normal distribution, $n = n_1 + n_2$ is the total sample size, and $c = n_1/n$. This cutoff can be derived by applying a standard central limit theorem for two-sample U-statistics to the Kendall's tau statistic. The cutoff values for the A vs. C and R vs. C group contrasts were 0.4032 and 0.4217, respectively.

Statistical methods for prediction models

Connectivity of the selected tracts from the feature selection process was used to predict the LFDRS and DOSPERT scores. Connectivity and total LFDRS variables were square root- and log-transformed, respectively, to reduce skewness. Ridge regression models were used to predict the response variables from the tract features, and leave-one-out cross validation was used to assess predictive ability. Standard leave-one-out cross-validation predictions were performed using the following process [for further details, see (Kriegeskorte 2015)]: data from a given subject was designated as a test set, while data from the remaining subjects were designated as the training set. The training set was used to estimate a prediction model, which was subsequently applied to the predictor variables of the test set to predict the response variable of the same set. This procedure was repeated n times, where n denotes the sample size, such that the data from each subject was evaluated once as the test set. Pearson's correlation between the observed and predicted response variables, denoted as r, was computed to assess model fit. For analyses comparing the predictive abilities of a base model and a full model, we computed the reduction in square root mean squared error (RMSE) as $100 \times (\psi_b - \psi_f)/\psi_b$, where ψ_b and ψ_f denote the RMSE of the reduced and full models. To assess the statistical significance of the prediction metrics (r and reduction in RMSE), we randomly permuted the subject labels 5000 times and computed the metrics for each permutation to obtain permutation distributions for the metrics. Permutation-based p values were then computed as the proportion of observations from the permutation distribution that exceeded the observed prediction metric (Nichols and Holmes 2002).

Results

Sample characteristics

Comparisons of demographic and cognitive characteristics between the three risk-taking preference groups can be found in Table 1. F tests and chi-square tests were used to test for the presence of any differences in group means and sample proportions between the continuous and categorical sample characteristics, respectively. Only sex ($p = 0.03$) and the overall accuracy from the WCST significantly differed between the three groups ($p = 0.04$). Six participants were excluded from the connectome analyses due to errors during DTI processing. The results of the sample characteristic comparisons were the same for the reduced sample ($n = 44$) used for the connectome analyses.

Two-sample t tests assuming unequal variances were used to test if any pairs of risk-taking preference groups differed on the IGT, BART, and cognitive arousal z-scores. The average scores by group and significant pairwise differences are presented in Fig. 1. Both A and R groups had significantly higher average BART scores than the C group, and the A group had significantly higher average cognitive arousal scores, with a trend ($p < 0.10$) for higher IGT scores than both R and C groups.

The DOSPERT questionnaire was mailed out to participants who had usable DTI data for the connectome analyses ($n = 44$). Thirty-five participants completed the questionnaire; two of those participants were missing risk-taking preference classifications due to technical errors while recording their gambling task behavior data. A significant difference between the three risk-taking preference groups was observed only in the health/safety domain score of DOSPERT ($p = 0.02$). No significant differences in sample characteristics were observed between participants who completed DOSPERT and those who did not; additionally, no significant differences in LFDRS scores were observed between the three groups.

Description of group contrast connectome features

The majority of tracts from A vs. C (56 out of 72) and R vs. C (71 out of 85) contrasts had positive tau statistics, indicating that participants from the A and R groups had significantly higher connectivity for those tracts than participants from the C group. All but one of the 17 overlapping tracts from the comparisons of A vs. C and R vs. C had positive tau statistics. To visualize the connectivity features, tracts selected as features from comparisons of the number of connections within the A vs. C and R vs. C

Table 1 Sample characteristics

	A ($n=15$)	R ($n=16$)	C ($n=19$)	F or χ^2 test, $df1$, $df2$ (p)
Age (years)	70.53 (4.05)	70.59 (4.27)	72.21 (6.58)	0.59, 2, 47 (0.56)
Sex [n female (%)]	9 (60)	10 (62.5)	18 (95)	**6.87, 2 (0.03)**
Education (years)	16.60 (2.26)	17.31 (2.44)	15.58 (2.43)	2.34, 2, 47 (0.11)
MOCA	27.33 (1.84)	28.06 (1.81)	27.74 (1.37)	0.75, 2, 47 (0.48)
Cognitive control	0.49 (0.41)	0.48 (0.40)	0.47 (0.47)	0.02, 2, 47 (0.98)
Working memory	0.292 (0.72)	0.29 (0.53)	0.509 (0.57)	0.75, 2, 47 (0.48)
Delay recall	11.33 (2.77)	10.50 (3.22)	10.26 (1.76)	0.75, 2, 47 (0.48)
Cortical thickness	2.44 (0.10)	2.46 (0.10)	2.48 (0.11)	0.43, 2, 47 (0.65)
Reasoning	0.68 (0.04)	0.69 (0.05)	0.65 (0.06)	**3.38, 2, 47 (0.04)**
Log Total LFDRS	2.06 (0.68)	1.93 (0.50)	1.89 (0.51)	0.41, 2, 47 (0.67)
IGT z score	0.51 (1.39)	− 0.27 (0.73)	− 0.20 (0.69)	3.15, 2, 47 (0.05)
BART z score	0.63 (0.68)	0.67 (0.52)	− 1.03 (0.56)	**47.77, 2, 47 (< 0.0001)**
Cognitive arousal z score	0.98 (0.85)	− 0.62 (0.83)	− 0.24 (0.69)	**17.52, 2, 47 (< 0.0001)**
	A ($n=8$)	R ($n=14$)	C ($n=11$)	
DOSPERT total score	73 (15.04)	63.38 (10.71)	68.45 (13.52)	1.43, 2, 31 (0.25)
DOSPERT ethical score	9.25 (2.38)	8.15 (2.27)	8.36 (2.20)	0.61, 2, 31 (0.54)
DOSPERT financial score	11.38 (3.46)	11.15 (3.93)	11.73 (3.10)	0.08, 2, 31 (0.92)
DOSPERT health score	11.88 (4.64)	7.62 (1.66)	9.36 (3.58)	**4.17, 2, 31 (0.02)**
DOSPERT recreational score	10.75 (5.78)	8.31 (4.33)	10.45 (5.07)	0.82, 2, 31 (0.44)
DOSPERT social score	29.38 (7.42)	28.46 (6.83)	28.64 (6.10)	0.05, 2, 31 (0.95)

A, group preferring ambiguity-based decision-making; R, group preferring risk-based DM; C, group with no apparent decision-making preference; SD, standard deviation; *F, F* test statistic; χ^2, Chi-square test statistic; df, degrees of freedom; p, p value; MOCA, Montreal Cognitive Assessment; WCST, Wisconsin Card Sorting Task; LFDRS, Lichtenberg Financial Decision-Making Rating Scale; IGT, Iowa Gambling Task; BART, Balloon Analogue Risk Task; DOSPERT, Likelihood Rating from the Domain-Specific Risk-Taking scale

Bold values indicate $p < 0.05$

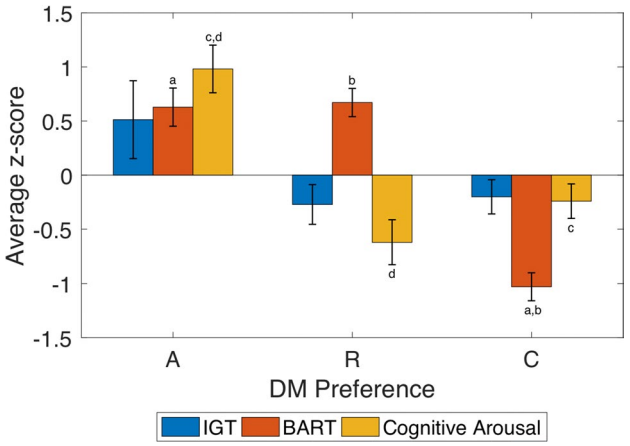

Fig. 1 Comparison of standardized IGT, BART, and cognitive arousal scores between the A, R, and C groups. Superscripts a, b, c, and d denote significant pairwise mean differences at the 0.05 level. The differences between A and R/C groups for IGT are significant at level 0.10

contrasts are presented as glass brain plots in Fig. 2. MNI space coordinates for the Desikan-Killiany atlas brain regions can be found in Supplementary Table 4.

Out of the unique A vs. C tracts, the largest hubs among the tracts with a positive tau statistic were centered in the right caudate with six connections, and the left caudate and left rostral anterior cingulate (RAC), each consisting of five connections. The largest hubs among the tracts with a negative tau statistic were centered in the right middle temporal gyrus (MTG) with five connections and the brain stem and right pallidum, each consisting of three connections.

Among the unique R vs. C tracts, the largest hub among the tracts with a positive tau statistic were centered in the right frontal pole (FP) with nine connections and the right caudal anterior cingulate (CAC), left pericalcarine, and right superior frontal gyrus (SFG), each consisting of five connections. The largest hubs among the tracts with negative tau statistics were centered in the left pallidum with three connections.

Finally, among the shared tracts from the A vs. C and R vs. C contrasts, the largest hubs among the tracts with a positive tau statistic were centered in the right thalamus and right putamen, each with three connections; however, only a single tract, connecting the right temporal pole to the right MTG, was comprised of the shared features with a negative

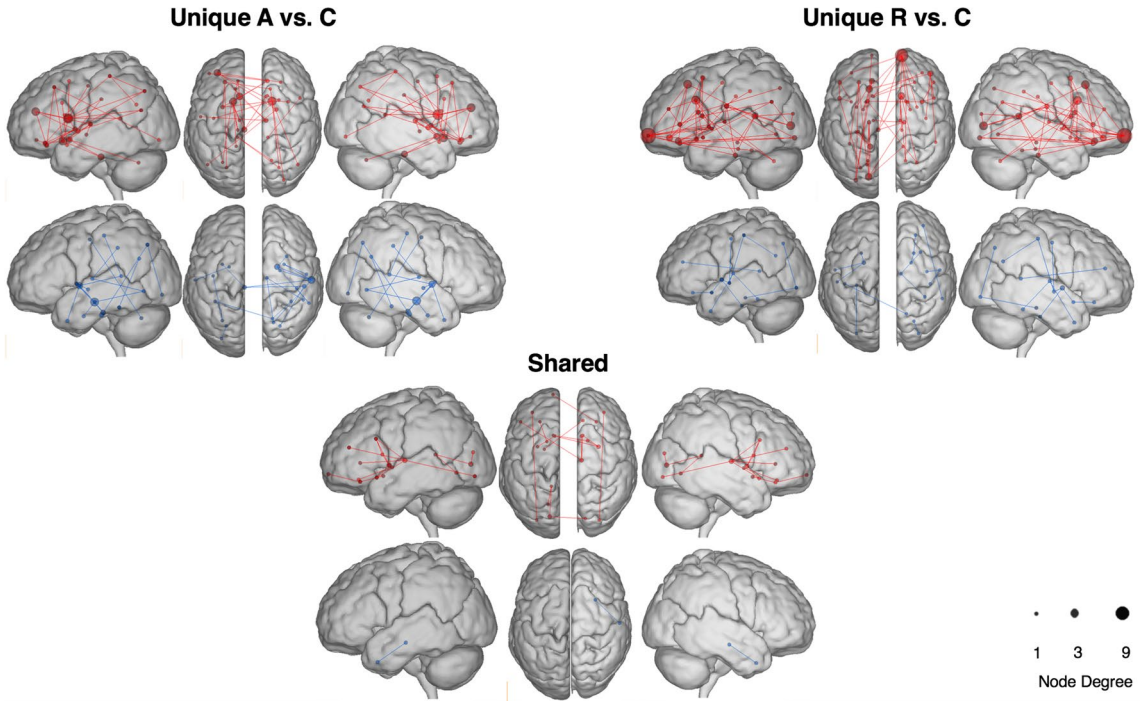

Fig. 2 Glass brain plots of unique A vs. C, unique R vs. C, and shared tracts selected during NC feature selection. Red (blue) signifies tracts with positive (negative) tau statistics

tau statistic. The signs of the tau statistics of the shared tracts were the same over the two group contrasts.

Relationships between group-based connectome features and everyday decision-making scores

In models using the connectivity features to predict everyday decision-making scores (Fig. 3), the total A vs. C features significantly predicted LFDRS ($r = 0.55$, $p = 0.006$) and showed a trend for predicting DOSPERT total score ($r = 0.29$, $p = 0.12$). The total A vs. C features also predicted significantly, or with a trend towards significance, the DOSPERT scores from the financial ($r = 0.42$, $p = 0.045$), health/safety ($r = 0.46$, $p = 0.03$), and social domains ($r = 0.38$, $p = 0.06$). Neither the shared features nor the total R vs. C were predictive of the everyday decision-making scores.

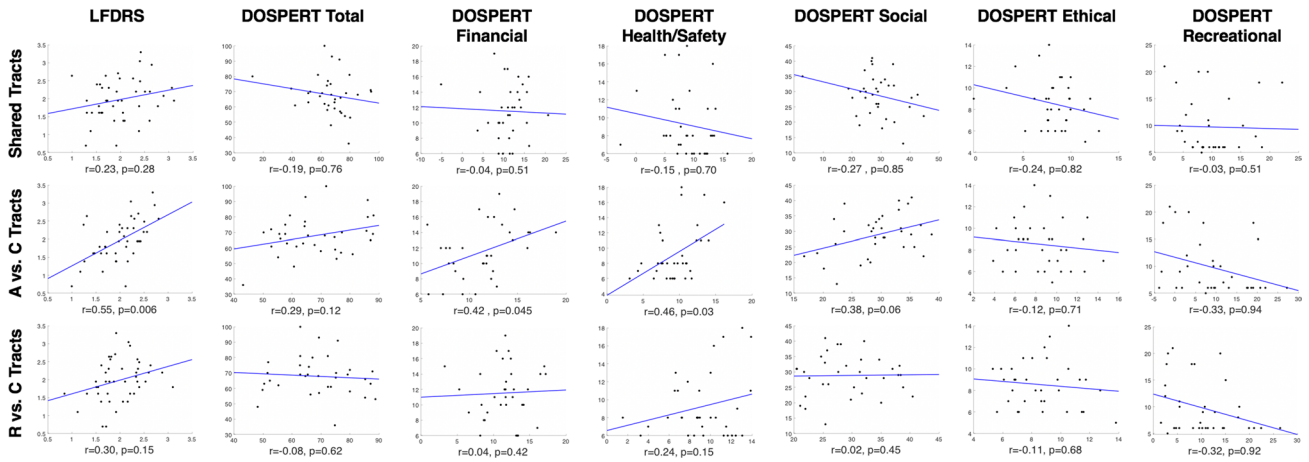

Fig. 3 Scatter plots of observed (*y* axis) vs. predicted (*x* axis) decision-making scores from models using NC from A vs. C, R vs. C, and shared tracts to predict decision-making, overlaid with blue best-fit linear regression lines

To analyze the unique contributions from A vs. C and R vs. C connectivity features in the prediction of LFDRS and DOSPERT scores, we compared full models composed of all connectivity features from the A vs. C or R vs. C contrast against a reduced model where the shared tracts common to the A vs. C or R vs. C connectivity features were used as predictors of LFDRS and DOSPERT total and domain scores (Table 2). Addition of the unique tracts from the A vs. C features to the reduced model with only shared tracts significantly improved the prediction accuracy of LFDRS (reduction in RMSE = 26%, $p = 0.02$), and DOSPERT total score (reduction in RMSE = 32%, $p = 0.04$), as well as several DOSPERT domain scores (: reduction in financial RMSE = 38%, $p = 0.02$; reduction in health/safety RMSE = 40%, $p = 0.02$; reduction in social RMSE = 40%, $p = 0.01$).

To evaluate the contribution of the connectivity features to the prediction of LFDRS and DOSPERT scores beyond that of sample characteristics (i.e., age, sex, years of education, MoCA, cognitive control, working memory, delayed recall, cortical thickness, and reasoning), we compared a full model of connectivity features plus sample characteristics as predictors of LFDRS and DOSPERT scores to a reduced model using only sample characteristics as the predictors (Table 3). Addition of the total A vs. C features to the reduced model significantly improved the prediction of LFDRS (reduction in RMSE = 14%, $p = 0.02$) and several domain scores of DOSPERT (reduction in financial RMSE = 6%, $p = 0.05$; reduction in health/safety RMSE = 11%, p = 0.02).

Table 2 Percent reduction in root mean squared error (RMSE) from adding unique tracts to shared tracts in prediction models

	Shared tracts + unique A vs. C tracts	Shared tracts + unique R vs. C tracts
LFDRS total score	25.8% (0.02)	8.6% (0.13)
DOSPERT total score	32.1% (0.04)	17.9% (0.21)
DOSPERT financial score	37.5% (0.02)	20.2% (0.18)
DOSPERT health/safety score	40.4% (0.02)	28.6% (0.07)
DOSPERT ethical score	3% (0.39)	13.2% (0.29)
DOSPERT social score	40.2% (0.01)	22.6% (0.14)
DOSPERT recreational score	− 57.2% (0.97)	− 34.4% (0.96)

Results presented as % reduction in MSE (*p* value)

A, group preferring ambiguity-based decision-making; R, group preferring risk-based DM; C, group with no apparent decision-making preference; LFDRS, Lichtenberg Financial Decision-Making Rating Scale; DOSPERT, Likelihood Rating from the Domain-Specific Risk-Taking scale

Table 3 Reduction in mean squared error (MSE) from adding NC features to sample characteristics in prediction models

	Sample chars. + A vs. C tracts	Sample chars. + R vs. C tracts
LFDRS total score	13.7% (0.02)	− 12.5% (0.28)
DOSPERT total score	− 5.5% (0.12)	− 31.1% (0.52)
DOSPERT financial score	5.9% (0.05)	− 26.4% (0.44)
DOSPERT health/safety score	11.2% (0.02)	− 10.4% (0.20)
DOSPERT ethical score	− 62.73% (0.80)	− 44.1% (0.72)
DOSPERT social score	− 2.4% (0.10)	− 26% (0.46)
DOSPERT recreational score	− 82% (0.92)	− 67.6% (0.91)

Results presented as % reduction in MSE (*p* value)

A, group preferring ambiguity-based decision-making; R, group preferring risk-based DM; C, group with no apparent decision-making preference; LFDRS, Lichtenberg Financial Decision-Making Rating Scale; DOSPERT, Likelihood Rating from the Domain-Specific Risk-Taking scale

Discussion

In the current study, we identified three groups with distinct risk-taking preference: one with ambiguity preference (A), indexed by high performance on IGT and BART, as well as greater cognitive arousal after the tasks; one with risk-seeking preference (R), indexed by high performance on BART and greater cognitive arousal, but low performance on IGT; and one that lacked a clear risk-taking preference (C), indexed by low performance on both tasks but high excitement. Next, by comparing the A or R group with C in whole-brain connectomes, we revealed three types of connectomes: (1) unique tracts differentiating A from C, indexed by more connections seeded in the bilateral caudate and left RAC and fewer connections seeded in right MTG; (2) unique tracts differentiating R from C, indexed by more connections in the right FP, right CAC, left pericalcarine, and right SFG, and fewer connections seeded in left pallidum; and (3) shared tracts underlying A and R compared to C, indexed by more connections seeded in the right thalamus and putamen. Finally, among these tracts, connectivity from those differentiating A from C (particularly unique tracts) demonstrated significant and robust predictive power for the financial and health domains of everyday decision-making capacity under different types of model comparisons.

Consistent with our hypothesis based on the functional brain system involved in decision-making, shared tracts between A and R groups were primarily localized in the basal ganglia, a region associated with coordinating different types of decision-making processes (Ding and Gold 2013). Tract differences in these two groups stemmed primarily from differential involvement of dorsal (i.e., RAC in A) and ventral frontal regions (i.e., FP in R). Dorsal frontal regions

are considered part of the reflective system, while ventral frontal regions are considered part of the impulsive system underlying decision-making (Schiebener and Brand 2015). Of note, hub regions supporting the differences between individuals with a clear risk-taking preference (A or R) compared to those without one (C) were right-hemisphere dominant. These findings agree with existing literature that indicates age-associated brain changes are more prominent in the right hemisphere (Grady et al. 1994). Additionally, our findings suggest that the lower white matter streamline of the right hemisphere connectome may contribute to the control group's failure to establish a clear risk-taking preference compared to the other two groups.

In contrast to our hypothesis pertaining to the potential role of shared tracts in predicting everyday decision-making, A vs. C contrast connectomes, particularly the unique features, appear to be particularly relevant to everyday decision-making capacity, particularly financial and health domains, which are of increasing concern in old age. Of note, a previous study found that white matter tracts of parietal and temporal regions were associated with financial literacy in older adults (Han et al. 2016). Financial literacy refers to the ability to understand, access, and utilize monetary information, which is more strongly related to memory and learning (Huston 2010); however, in the current study, we examined perceived financial decision-making capacity, using LFDRS and DOSERPT to assess domains of financial situational awareness, psychological vulnerability regarding finances, susceptibility to undue influence and/or exploitation, as well as likelihood of taking financial risk, all of which are more related to self-value and control (Lichtenberg et al. 2018b). Regarding health-related decision-making, a previous task-based fMRI study with predominantly younger adults found that multiple frontal regions responded to negative messages concerning health (e.g., smoking) (Falk et al. 2016). Here, we narrowed down the neural correlates of health/safety-related decision-making to dorsal frontal regions in old age.

One point we would like to highlight is that we assessed a particularly healthy older adult sample.

This was evident, for example, in individuals without a clear risk-taking pattern (group C), where stronger white matter streamlines were seeded in posterior regions, such as MTG, which is part of the semantic network (Acheson and Hagoort 2013). Consequently, the relative integrity of these regions may help temporarily protect group C from exhibiting deficits in everyday decision-making. Additionally, the cognitive health of this sample may explain the lack of significant relationships between cognitive domains and risk-taking patterns, with the exception of reasoning. That is, individuals without clear decision-making patterns (C) may still self-perceive relatively normal financial decision-making capacity due to intact cognitive performance across multiple domains.

Currently, the most common approach to identify neural correlates of decision-making capacity is to select neural differences between clinical phenotypes (e.g., Alzheimer's disease vs. cognitively typical older adults) as the neural candidates to explain certain types of decision-making capacity (Griffith et al. 2010; Stoeckel et al. 2013; Gerstenecker et al. 2017). This approach is implemented under the assumption that neurodegeneration contributes to impaired decision-making capacity. Nonetheless, such a process propagates several limitations; regions supporting decision-making capacity, predominantly prefrontal cortices, are not necessarily affected during the early stages of neurodegeneration—the compensatory role of these regions may instead interfere with the interpretation (Cabeza and Dennis 2013). Furthermore, one must assume normality of everyday decision-making capacity among older adults absent cognitive impairment while ignoring cumulative evidence that older adults, in general, are at high risk for poor decision-making capacity (Tymula et al. 2013). Notably, our implementation of a different approach identified a connectome map seeded in dorsal frontal and basal ganglia regions underlying ambiguity-based risk-taking preference, which, in turn, was associated with financial- and health-related decision-making capacity in a sample of cognitively and physically healthy older adults.

To validate our findings several limitations in the current design will need to be addressed. First, we did not have a younger comparison group; thus, it is unclear whether the same connectome map derived from the A vs. C contrast exists in younger adults. Our hypothesis that a functional neural map underlies the decision-making process was based on evidence from studies that included younger adults (Schiebener and Brand 2015). We therefore propose that the current results may be valid across adulthood. By comparing our sample to younger adults, we would aim to identify tracts that are particularly vulnerable to aging and may be more sensitive as therapeutic targets for addressing financial exploitation in older adults. Second, whether our process of identifying risk-taking patterns was exhaustive needs to be validated in a larger sample. For example, a bias for temporal discounting (i.e., the preference for a small, immediate reward over a large, delayed reward) may be hidden in any of the risk-taking preferences we evaluated (i.e., good or mediocre performance in IGT, but mediocre or poor in BART) (Frost and McNaughton 2017). Relevantly, we were not able to determine whether there exists a group of individuals who can switch flexibly between risk-taking preference, depending on the specific context. A future study that is able to determine the existence of such groups and their associated brain profiles would likely provide further therapeutic insight. Third, we were unable to account for white matter hyperintensities because we did not collect FLAIR data

during fMRI data acquisition. However, we did have a healthy older adult sample without major neurologic and vascular diseases. Fourth, additional dynamic factors that are particularly relevant in old age, such as social connectedness or interpersonal relationships (Krueger and Meyer-Lindenberg 2019), may also be related to both risk-taking preference and everyday decision-making. Accordingly, these factors warrant further examination in future studies to understand comprehensively the unique contribution of the brain map revealed here to everyday decision-making capacity. Of note, we found that the number of connections within ROI-to-ROI tracts provided superior prediction of everyday decision-making domains compared to other diffusion measures, such as mean FA or mean MD. These findings bolster existing literature on the interplay in younger populations between FA-based white matter tracts and risk-based decision-making (Kohno et al. 2017).

In summary, the present paper presents evidence of a white-matter neural profile that can predict different types of risk-taking preferences in older adults. Using an innovative approach that derives connectomes from risk-taking preference, we identified tracts in prefrontal cortex that discriminate ambiguity-seekers from those without a clear preference and significantly predict financial and health/safety decision-making capacity. Our findings extend existing literature on the relationship between white matter tracts and decision-making preference. Although it remains unclear whether age-associated physiological changes contribute to differences in these white- matter indices, the neural profile we describe here may offer insight into a generic white-matter mechanism related to changes in decision-making capacity prevalent in cognitive aging. Further examination of this potential mechanism in longitudinal studies of young and older populations will strengthen the discussion between researchers and clinicians on neurocognitive factors critical to therapeutic strategies that address behavioral changes in domains of decision-making instrumental to functional independence and identify individuals vulnerable to elder mistreatment.

Acknowledgements No conflict of interest to be disclosed. Data collection and paper development is funded by NIH/NIA R21AG053193, as well as University of Rochester Goergen Institute for Data Science Collaborative Pilot Aware Program in Health Analytics to F. Lin.

Funding Data collection and paper development is funded by NIH/NIA R21AG053193, as well as University of Rochester Goergen Institute for Data Science Collaborative Pilot Aware Program in Health Analytics to F. Lin.

Compliance with ethical standards

Conflict of interest The authors declare that they have no conflict of interest.

Ethical approval All procedures performed in studies involving human participants were approved by the Institutional Review Board of University of Rochester and in accordance with the 1964 Helsinki Declaration and its later amendments or comparable ethical standards.

Informed consent All participants provided written consent.

References

Acheson DJ, Hagoort P (2013) Stimulating the brain's language network: syntactic ambiguity resolution after TMS to the inferior frontal gyrus and middle temporal gyrus. J Cogn Neurosci 25:1664–1677

Blais A-R, Weber EU (2006) A domain-specific risk-taking (DOSPERT) scale for adult populations. Judgm Decis Mak 1:33–47

Cabeza R, Dennis NA (2013) Frontal lobes and aging: deterioration and compensation. In: Stuss DT, Knight RT (eds) Principles of frontal lobe function, 2nd Edition, pp 628–652. Oxford University Press, Oxford

Desikan RS, Segonne F, Fischl B, Quinn BT, Dickerson BC, Blacker D, Buckner RL, Dale AM, Maguire RP, Hyman BT, Albert MS, Killiany RJ (2006) An automated labeling system for subdividing the human cerebral cortex on MRI scans into gyral based regions of interest. Neuroimage 31:968–980

Ding L, Gold JI (2013) The basal ganglia's contributions to perceptual decision making. Neuron 79:640–649

Falk EB, O'Donnell MB, Tompson S, Gonzalez R, Dal Cin S, Strecher V, Cummings KM, An L (2016) Functional brain imaging predicts public health campaign success. Soc Cogn Affect Neurosci 11:204–214

Frost R, McNaughton N (2017) The neural basis of delay discounting: a review and preliminary model. Neurosci Biobehav Rev 79:48–65

Gerstenecker A, Hoagey DA, Marson DC, Kennedy KM (2017) White matter degradation is associated with reduced financial capacity in mild cognitive impairment and Alzheimer's disease. J Alzheimers Dis 60:537–547

Giedd JN, Rapoport JL (2010) Structural MRI of pediatric brain development: what have we learned and where are we going? Neuron 67:728–734

Grady CL, Maisog JM, Horwitz B, Ungerleider LG, Mentis MJ, Salerno JA, Pietrini P, Wagner E, Haxby JV (1994) Age-related changes in cortical blood flow activation during visual processing of faces and location. J Neurosci 14:1450–1462

Griffith HR, Stewart CC, Stoeckel LE, Okonkwo OC, den Hollander JA, Martin RC, Belue K, Copeland JN, Harrell LE, Brockington JC, Clark DG, Marson DC (2010) Magnetic resonance imaging volume of the angular gyri predicts financial skill deficits in people with amnestic mild cognitive impairment. J Am Geriatr Soc 58:265–274

Hampton WH, Alm KH, Venkatraman V, Nugiel T, Olson IR (2017) Dissociable frontostriatal white matter connectivity underlies reward and motor impulsivity. Neuroimage 150:336–343

Han SD, Boyle PA, Arfanakis K, Fleischman D, Yu L, James BD, Bennett DA (2016) Financial literacy is associated with white matter integrity in old age. Neuroimage 130:223–229

Huston SJ (2010) Measuring financial literacy. J Consum Affairs 44:296–316

Kohno M, Morales AM, Guttman Z, London ED (2017) A neural network that links brain function, white-matter structure and risky behavior. Neuroimage 149:15–22

Koscielniak M, Rydzewska K, Sedek G (2016) Effects of age and initial risk perception on balloon analog risk task: the mediating role of

processing speed and need for cognitive closure. Front Psychol 7:659
Kriegeskorte N (2015) Crossvalidation in brain imaging analysis. Biorxiv. https://doi.org/10.1101/017418
Krueger F, Meyer-Lindenberg A (2019) Toward a model of interpersonal trust drawn from neuroscience, psychology, and economics. Trends Neurosci 42:92–101
Lee KA, Hicks G, Nino-Murcia G (1991) Validity and reliability of a scale to assess fatigue. Psychiatry Res 36:291–298
Leong JK, Pestilli F, Wu CC, Samanez-Larkin GR, Knutson B (2016) White-matter tract connecting anterior insula to nucleus accumbens correlates with reduced preference for positively skewed gambles. Neuron 89:63–69
Li SC, Lindenberger U, Hommel B, Aschersleben G, Prinz W, Baltes PB (2004) Transformations in the couplings among intellectual abilities and constituent cognitive processes across the life span. Psychol Sci 15:155–163
Lichtenberg PA, Ficker LJ, Rahman-Filipiak A (2016) Financial decision-making abilities and financial exploitation in older African Americans: preliminary validity evidence for the lichtenberg financial decision rating scale (LFDRS). J Elder Abuse Neglect 28:14–33
Lichtenberg PA, Teresi JA, Ocepek-Welikson K, Eimicke JP (2017) Reliability and validity of the lichtenberg financial decision screening scale. Innov Aging 2017:1
Lichtenberg PA, Gross E, Ficker LJ (2018a) Quantifying risk of financial incapacity and financial exploitation in community-dwelling older adults: utility of a scoring system for the lichtenberg financial decision-making rating scale. Clin Gerontol 2017:1–15
Lichtenberg PA, Ocepek-Welikson K, Ficker LJ, Gross E, Rahman-Filipiak A, Teresi JA (2018b) Conceptual and empirical approaches to financial decision-making by older adults: results from a financial decision-making rating scale. Clin Gerontol 41:42–65
Liebherr M, Schiebener J, Averbeck H, Brand M (2017) Decision making under ambiguity and objective risk in higher age—a review on cognitive and emotional contributions. Front Psychol 8:2128
Mata R, Josef AK, Samanez-Larkin GR, Hertwig R (2011) Age differences in risky choice: a meta-analysis. Ann N Y Acad Sci 1235:18–29
Mikels JA, Cheung E, Cone J, Gilovich T (2013) The dark side of intuition: aging and increases in nonoptimal intuitive decisions. Emotion 13:189–195
Monje M (2018) Myelin plasticity and nervous system function. Annu Rev Neurosci 41:61–76
Nichols TE, Holmes AP (2002) Nonparametric permutation tests for functional neuroimaging: a primer with examples. Hum Brain Mapp 15:1–25
Samanez-Larkin GR, Kuhnen CM, Yoo DJ, Knutson B (2010) Variability in nucleus accumbens activity mediates age-related suboptimal financial risk taking. J Neurosci 30:1426–1434
Schiebener J, Brand M (2015) Decision making under objective risk conditions-a review of cognitive and emotional correlates, strategies, feedback processing, and external influences. Neuropsychol Rev 25:171–198
Spreng RN, Cassidy BN, Darboh BS, DuPre E, Lockrow AW, Setton R, Turner GR (2017) Financial exploitation is associated with structural and functional brain differences in healthy older adults. J Gerontol A Biol Sci Med Sci 72:1365–1368
Stoeckel LE, Stewart CC, Griffith HR, Triebel K, Okonkwo OC, den Hollander JA, Martin RC, Belue K, Copeland JN, Harrell LE, Brockington JC, Clark DG, Marson DC (2013) MRI volume of the medial frontal cortex predicts financial capacity in patients with mild Alzheimer's disease. Brain Imaging Behav 7:282–292
Tymula A, Rosenberg Belmaker LA, Ruderman L, Glimcher PW, Levy I (2013) Like cognitive function, decision making across the life span shows profound age-related changes. Proc Natl Acad Sci USA 110:17143–17148
Zamarian L, Weiss EM, Delazer M (2011) The impact of mild cognitive impairment on decision making in two gambling tasks. J Gerontol B Psychol Sci Soc Sci 66:23–31
Zhang Z, Descoteaux M, Zhang J, Girard G, Chamberland M, Dunson D, Srivastava A, Zhu H (2018) Mapping population-based structural connectomes. Neuroimage 172:130–145